NACA RM L53D03

7418

NACA

RESEARCH MEMORANDUM

AERODYNAMIC CHARACTERISTICS AT MACH NUMBER 4.04 OF

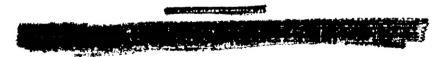A RECTANGULAR WING OF ASPECT RATIO 1.33 HAVING

A 6-PERCENT-THICK CIRCULAR-ARC PROFILE AND A

30-PERCENT-CHORD FULL-SPAN

TRAILING-EDGE FLAP

By Robert W. Dunning and Edward F. Ulmann

Langley Aeronautical Laboratory
Langley Field, Va.

NATIONAL ADVISORY COMMITTEE
FOR AERONAUTICS
WASHINGTON
May 29, 1953

CONFIDENTIAL

NATIONAL ADVISORY COMMITTEE FOR AERONAUTICS

RESEARCH MEMORANDUM

AERODYNAMIC CHARACTERISTICS AT MACH NUMBER 4.04 OF

A RECTANGULAR WING OF ASPECT RATIO 1.33 HAVING

A 6-PERCENT-THICK CIRCULAR-ARC PROFILE AND A

30-PERCENT-CHORD FULL-SPAN

TRAILING-EDGE FLAP

By Robert W. Dunning and Edward F. Ulmann

SUMMARY

Force and moment measurements were made at a Mach number of 4.04 and a Reynolds number of 8.0×10^6 on a rectangular-plan-form wing of aspect ratio 1.33 having a 6-percent-thick circular-arc profile and a 30-percent-chord full-span trailing-edge flap. The results are compared with two-dimensional results previously obtained on the same airfoil-flap configuration at the same Mach number and with the predictions of NACA TN 1708. The comparison indicates that at zero angle of attack and flap angle, the two-dimensional slope parameters and the slope parameters of the wing and control panel can be predicted very well by the method of NACA TN 1708. The theoretical slope characteristics can be used to predict coefficient values with good accuracy throughout most of the range of angles investigated except in the case of the slope of the hinge-moment coefficient variation with flap angle.

INTRODUCTION

At the present time the Langley Aeronautical Laboratory is conducting a program to determine the aerodynamic characteristics of controls at supersonic speeds. The present report gives results at a Mach number of 4.04 of that part of the program concerned with flap controls at Mach numbers from 1.62 to 6.9. Other phases of this program include investigation of wing-tip-control and spoiler characteristics. Previous work consisted of two-dimensional pressure distributions and schlieren photographs of the flow over 6- and 9-percent-thick symmetrical circular-arc

CONFIDENTIAL

airfoils with 30-percent-chord trailing-edge flaps at Mach numbers
of 1.62 to 2.40 and Reynolds numbers of about 1×10^6 and at a Mach number
of 4.04 and Reynolds numbers of 5.0×10^6 to 8.4×10^6 (refs. 1, 2, and 3).
The results of the work at the lower Mach numbers and Reynolds numbers
(refs. 1 and 2) indicated that laminar separation occurred upstream of
the trailing-edge flap and resulted in breaks or shifts in the section
force and moment curves that might result in undesirable stability and
control characteristics. The tests at a Mach number of 4.04 (ref. 3)
showed that viscous effects, at Reynolds numbers from 5.0×10^6 to
8.4×10^6, had only minor effects on the aerodynamic coefficients of the
wing and of the trailing-edge control, probably because the boundary
layer was largely turbulent. This investigation also showed that the
two-dimensional-wing and control characteristics at a Mach number of 4.04
can be predicted very accurately by the shock-expansion method. The
Busemann second-order airfoil theory gave good predictions of the airfoil
characteristics but only fair predictions of the control characteristics.

The present tests on a rectangular wing of aspect ratio 1.33 having
the same 6-percent-thick airfoil section and trailing-edge-flap config-
uration as one of the models of references 2 and 3 were made to compare
the three-dimensional-wing and control characteristics with the results
of reference 3 and to assess the accuracy of available theoretical methods
for predicting the tip effects on rectangular wings. The tests were
conducted at a Mach number of 4.04 and a Reynolds number of 8.0×10^6,
based on wing chord, in the Langley 9- by 9-inch Mach number 4 blowdown
jet.

SYMBOLS

Moments are presented about the wind or stability axes.

M   free-stream Mach number

q   free-stream dynamic pressure

c   wing chord, 5.164 in.

b   wing span, twice semispan, 6.860 in.

b_f flap span, 3.430 in.

S   semispan wing area, 17.713 sq in.

c_f flap chord, 1.549 in.

r   wing-profile radius, 21.597 in.

see fig. 3

α wing angle of attack

δ flap deflection relative to chord of wing, positive downward

R Reynolds number based on wing chord

L lift of semispan wing

D drag of semispan wing

M' pitching moment of semispan wing about midchord

H hinge moment of semispan flap about hinge line

B bending moment due to lift of semispan wing about the wing root

L' rolling moment about the wing root due to the increment of lift from the deflection of one flap

C_L lift coefficient, L/qS

C_D drag coefficient, D/qS

$C_{m_{0.5}}$ pitching-moment coefficient, M'/qSc

C_h flap hinge-moment coefficient, $H/qc_f^2 b_f$

C_b wing-root bending-moment coefficient, B/qSb

C_l wing rolling-moment coefficient, $L'/2qSb$

L/D ratio of wing lift to wing drag

A aspect ratio

C_{L_α} variation of lift coefficient with angle of attack at zero lift coefficient, $\left(\dfrac{\partial C_L}{\partial \alpha}\right)_{\delta=0}$

C_{L_δ} variation of lift coefficient with flap deflection at zero lift coefficient, $\left(\dfrac{\partial C_L}{\partial \delta}\right)_{\alpha=0}$

C_{l_δ} variation of rolling-moment coefficient with flap deflection

at zero rolling-moment coefficient, $\left(\dfrac{\partial C_l}{\partial \delta}\right)_{\alpha=0}$

C_{h_δ} variation of flap-hinge-moment coefficient with flap deflec-

tion at zero flap deflection, $\left(\dfrac{\partial C_h}{\partial \delta}\right)_{\alpha=0}$

The subscripts outside the parentheses indicate the factors held constant during the measurement of the parameters.

APPARATUS

The tests were conducted in the Langley 9- by 9-inch Mach number 4 blowdown jet, which is described in reference 3. The settling-chamber pressure, which was held constant by a pressure-regulating valve, and the corresponding air temperature were continuously recorded on film. An external side-wall-mounted strain-gage balance was used to measure the normal force, chord force, pitching moment, and wing-root bending moment of the semispan model. Two strain-gage beams mounted within the wing were used to measure flap hinge moment. The model was mounted through a boundary-layer bypass plate (fig. 1), shaped to preserve the basic tunnel flow without introducing detrimental disturbances and located far enough from the tunnel wall to eliminate tunnel-wall boundary-layer effects. Balance deflection under load necessitated about 0.10-inch clearance all around the model at the root chord. Force tests of a rectangular wing equipped with pressure orifices on its surface just outboard and inboard of the gap at the wing root showed that air flow in and out of this 0.10-inch gap caused large changes in the wing-surface pressures which caused erroneous force and moment readings. A sliding-plate gap-sealing mechanism was therefore developed (figs. 1 and 2) which allowed the wing to move freely under load and reduced the effects of gap leakage to a negligible amount. Force tests were made which showed that the small friction existing between the sliding and stationary plates did not produce any measurable forces or moments.

MODELS

The model (fig. 3) was a semispan wing of rectangular plan form having a 30-percent-chord full-span trailing-edge flap, an aspect ratio

of 1.33, and a 6-percent-thick circular-arc profile with an included angle of 13.74° at the leading and trailing edges. The model had an unsealed gap of approximately 0.010 inch between the flap and the wing and was made of steel with a polished surface.

TESTS

Tests were made at a Reynolds number of 8.0×10^6 and a Mach number of 4.04 to obtain the lift, drag, pitching-moment, wing-root bending-moment, rolling-moment, and flap hinge-moment coefficients. The model angle of attack was varied from 0° to 10°, whereas the flap angle was varied from 12° to -12°. The tests were run at humidities below 5×10^{-6} pounds of water vapor per pound of dry air, which is believed to be low enough to eliminate any appreciable condensation effects.

PRECISION OF DATA

The uncertainties involved in measuring the model forces and moments and computing the aerodynamic coefficients and the center-of-pressure locations have been evaluated. The probable uncertainties in the data are listed below. The center-of-pressure inaccuracies are those for the centers of pressure at zero angle of attack and flap-deflection angle obtained by the slope method.

α . . . . ±0.1°
$\Delta\alpha$ . . . . ±0.05°
δ . . . . ±0.2°
C_L . . . . ±0.005
C_D . . . . ±0.001
C_m . . . . ±0.001
C_h . . . . ±0.002
C_b . . . . ±0.001
Chordwise c.p. . . . . ±0.01c
Spanwise c.p. . . . . ±0.01b

RESULTS

The figures presenting the experimental results do not contain the actual experimental points because of the simultaneous variation of angle
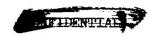
of attack and flap angle caused by deflection of the strain-gage beams;
for example, as the indicated angle of attack was varied from $0°$ to $10°$,
the deflection of the strain-gage beams allowed the model to move through
an additional angle of attack of about $0.3°$ and allowed the flap to
deflect as much as $0.7°$. Thus it was impossible to plot the data at
constant angle of attack or flap angle. The data curves presented herein
were obtained as follows. Angles of attack and flap-deflection angles
were corrected according to the recorded pitching moments and hinge
moments. The data were then plotted as a function of angle of attack,
each point having the corrected value of the flap-deflection angle noted
beside it. Coefficients for constant flap-deflection angles were obtained
by interpolation between the corrected flap-deflection-angle points.

Wherever possible in the presentation of the experimental results,
representative curves of the corresponding two-dimensional quantities
for the same airfoil-flap configuration at the same Mach number obtained
from reference 3 are included on the figures. Two-dimensional theoretical
values, available in reference 3, are not plotted in the interest of
clarity. Values of the lift-curve slope and some control-surface char-
acteristics for this wing at zero angle of attack and flap-deflection
angle computed by the method of reference 4 are compared with the experi-
mental values in table I. No accurate theoretical predictions of the
wing aerodynamic characteristics are available for the larger test angles.
Table I also contains experimental two-dimensional coefficients from
reference 3 and theoretical values of the same coefficients computed by
the method of reference 4 with $A = \infty$. The two-dimensional values of C_{l_δ}
were obtained by assuming that the lift was acting at the midsemispan
position. The equations of reference 4 were derived for flat-sided flaps
but, since the wing under test has only $4.13°$ change in slope over the
flap, it was assumed that the method would be applicable. The trailing-
edge angle used in the formulas of reference 4 was taken as the included
angle between straight lines drawn from the 70-percent-chord points on
the upper and lower airfoil surfaces to the trailing edge.

The lift curves for the wing are presented in figure 4. The drag
results are shown in figure 5 and the lift-drag ratios in figure 6. The
pitching-moment curves and the chordwise center-of-pressure locations
for the wing are compared with the two-dimensional results in figures 7
and 8, respectively. The hinge-moment curves and the values of C_{h_δ} at
zero flap-deflection angle are in figures 9 and 10, respectively. The
wing-root bending-moment coefficients, the wing rolling-moment coeffi-
cients, and the spanwise center-of-pressure locations are presented in
figures 11, 12, and 13, respectively. In the interest of clarity, the
spanwise center-of-pressure locations, as obtained from the faired data,
are indicated by symbols in figure 13.

DISCUSSION

The lift-curve slope and the control-surface characteristics of the test wing are compared in columns 1 and 2 of table I with the values obtained by the method of reference 4, which makes use of the Busemann third-order approximation for two-dimensional isentropic flow. The agreement between the experimental and the theoretical values is very good in all cases. Comparison of the experimental two-dimensional slope parameters from reference 3 (column 4, table I) and the theoretical values predicted by the method of reference 4, with $A = \infty$, (column 3, table I) also indicates very good agreement. Previous investigations (refs. 5 and 6) have shown that linearized theory gives poor prediction of trailing-edge control characteristics at high supersonic Mach numbers. Reference 3 showed that the Busemann second-order airfoil theory gave poor predictions of the two-dimensional control characteristics of the section used in the wing of these tests. Because of this poor agreement, predictions of the two- and three-dimensional control characteristics by these methods are not included. Experimentally, the differences between the two- and the three-dimensional results are small because of the relatively small tip losses at the test Mach number.

In general, the three-dimensional lift and moment characteristics of this configuration are more linear than the two-dimensional characteristics and are therefore more accurately predictable by slope methods. The theoretical slope characteristics given in table I can be used to predict coefficient values with good accuracy throughout most of the range of angles investigated except in the case of the slope of the hinge-moment coefficient variation with flap angle (fig. 9(b)), where the nonlinearities in the data become appreciable.

Comparison of the two- and three-dimensional lift coefficients (fig. 4) and the two- and three-dimensional drag coefficients (fig. 5) shows that the three-dimensional lift and drag coefficients are lower than the two-dimensional values except for the drag coefficient at low angles of attack and large flap deflections. In general, the resultant lift-drag ratios for the wing (fig. 6) are lower than the two-dimensional ratios.

The results of these tests showed that the trailing-edge flap did not exhibit any tendency toward regions of flap ineffectiveness, as was observed in the two-dimensional data for the same airfoil-flap configuration at lower Mach numbers and Reynolds numbers (refs. 1 and 2), but was continuously effective throughout the test angle range. This continuous effectiveness is in agreement with the results of the two-dimensional tests at a Mach number of 4.04 and Reynolds numbers of 5×10^6 and 8×10^6 on the same configuration (ref. 3).

CONCLUDING REMARKS

Aerodynamic coefficients obtained from force tests at a Mach number of 4.04 of a rectangular-plan-form wing of aspect ratio 1.33 with a 30-percent-chord trailing-edge full-span flap were compared with aerodynamic coefficients previously obtained by integration of two-dimensional pressure distributions obtained on the same wing at the same Mach number and Reynolds number and with theoretical predictions. The comparison indicated that at zero angle of attack and flap angle, the two-dimensional slope parameters and the slope parameters of the wing and control panel can be predicted very well by the theoretical method of NACA TN 1708. The theoretical slope characteristics can be used to predict coefficient values with good accuracy throughout most of the range of angles investigated, except in the case of the slope of the hinge-moment coefficient variation with flap angle. The three-dimensional lift and moments were found to be somewhat more linear than the two-dimensional data, although the differences between the two- and three-dimensional data were usually small.

Langley Aeronautical Laboratory,
    National Advisory Committee for Aeronautics,
        Langley Field, Va.

REFERENCES

1. Czarnecki, K. R., and Mueller, James N.: Investigation at Mach Number 1.62 of the Pressure Distribution Over a Rectangular Wing With Symmetrical Circular-Arc Section and 30-Percent-Chord Trailing-Edge Flap. NACA RM L9J05, 1950.

2. Czarnecki, K. R., and Mueller, James N.: Investigation at Supersonic Speeds of Some of the Factors Affecting the Flow Over a Rectangular Wing With Symmetrical Circular-Arc Section and 30-Percent-Chord Trailing-Edge Flap. NACA RM L50J18, 1951.

3. Ulmann, Edward F., and Lord, Douglas R.: An Investigation of Flow Characteristics at Mach Number 4.04 Over 6- and 9-Percent-Thick Symmetrical Circular-Arc Airfoils Having 30-Percent-Chord Trailing-Edge Flaps. NACA RM L51D30, 1951.

4. Tucker, Warren A., and Nelson, Robert L.: Theoretical Characteristics in Supersonic Flow of Constant-Chord Partial-Span Control Surfaces on Rectangular Wings Having Finite Thickness. NACA TN 1708, 1948.

5. Ivey, H. Reese: Notes on the Theoretical Characteristics of Two-Dimensional Supersonic Airfoils. NACA TN 1179, 1947.

6. Morrissette, Robert R., and Oborny, Lester F.: Theoretical Characteristics of Two-Dimensional Supersonic Control Surfaces. NACA TN 2486, 1951. (Supersedes NACA RM L8G12.)

TABLE I

COMPARISON OF EXPERIMENTAL DATA AT ZERO ANGLE OF ATTACK AND FLAP

ANGLE WITH THEORETICAL PREDICTIONS OBTAINED BY THE
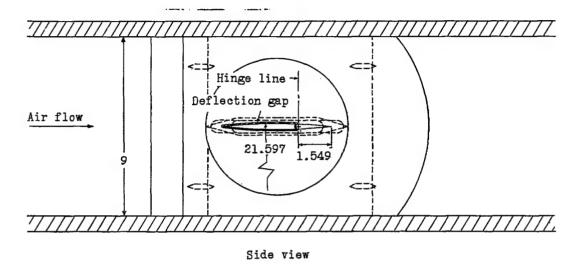
METHOD OF NACA TN 1708 (REF. 4)

Aerodynamic characteristics	Rectangular-wing results, A = 1.33		Two-dimensional results	
	Theoretical (ref. 4)	Experimental (this report)	Theoretical (ref. 4 with A = ∞)	Experimental (ref. 3)
c_{L_α}	0.017	0.018	0.019	0.020
c_{L_δ}	.0035	.0033	.0036	.0037
c_{l_δ}	.00042	.00045	[a].00045	[a].00046
$\left(c_{h_\delta}\right)_{\alpha=0}$	-.0054	-.0056	-.0060	-.0060

[a]Obtained by considering flap lift acting at the midsemispan position.

Hinge line

Deflection gap

Air flow

9

21.597   1.549

Side view

Hinge line

Hinge-moment beam location

Air flow

5.164

.010 gap

3.430

Boundary-layer bypass plate

9

Balance

NACA

Top view
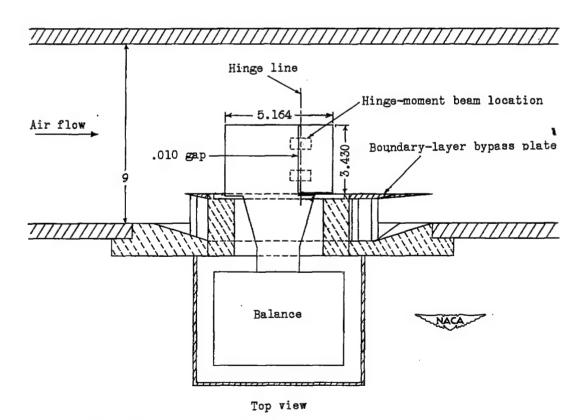
Figure 1.- Schematic diagram of test section of Langley 9- by 9-inch Mach
     number 4 blowdown jet and balance arrangement. All dimensions are in
     inches.
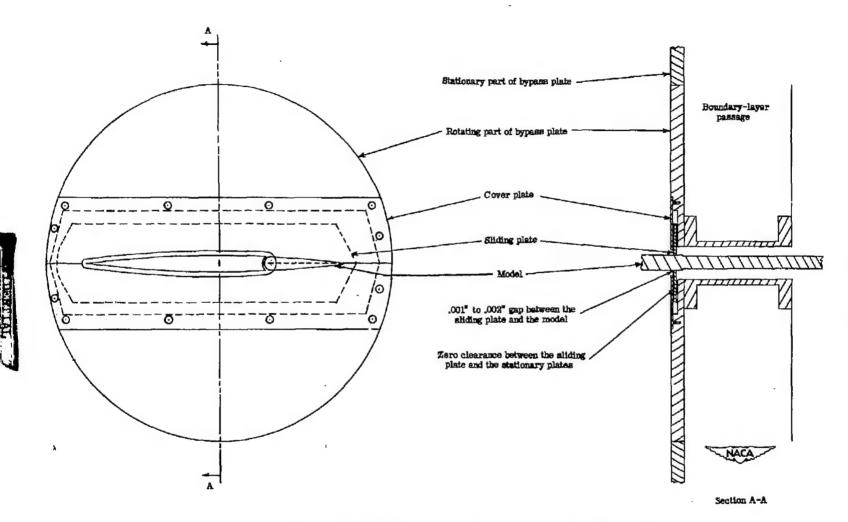
Figure 2.- Sliding-plate gap-sealing mechanism.
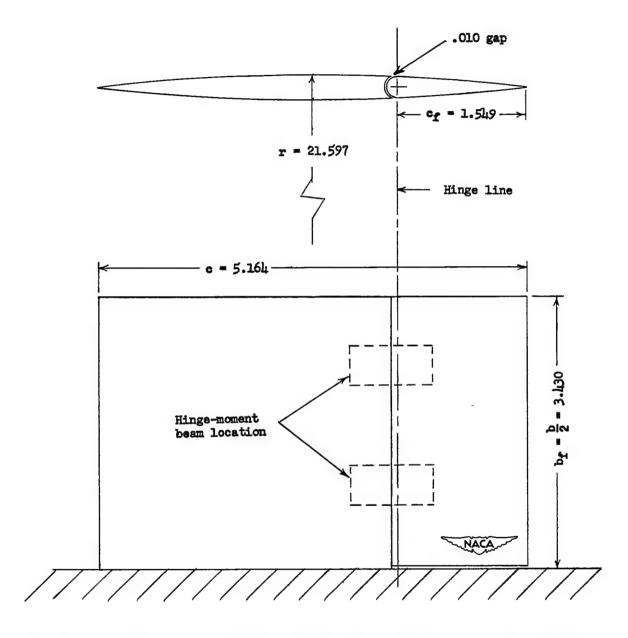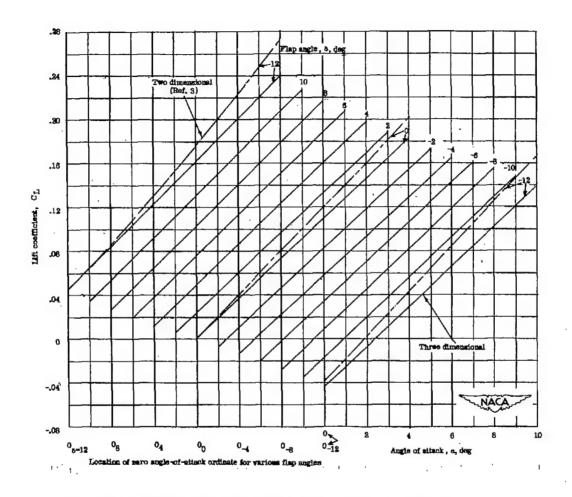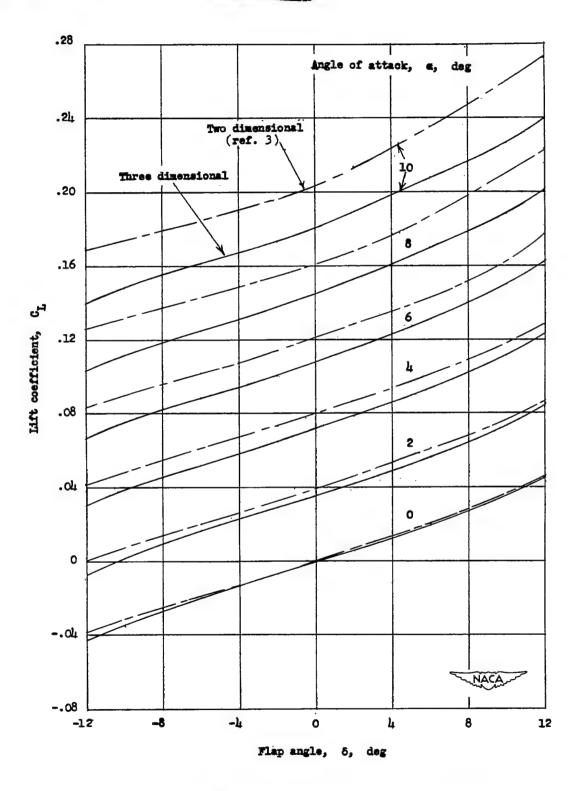
Figure 3.- Rectangular semispan model. All dimensions are in inches.

(a) Lift-coefficient variation with angle of attack.
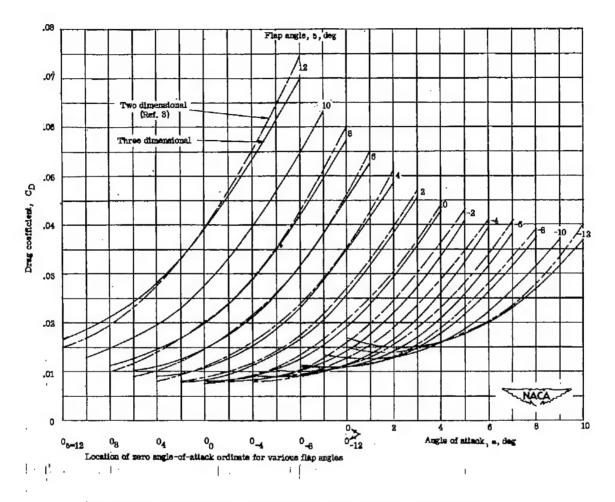
Figure 4.- The variation of lift coefficient with angle of attack and flap angle for a rectangular wing of aspect ratio 1.33 having a 6-percent-thick circular-arc profile and a 30-percent-chord full-span trailing-edge flap. $M = 4.04$; $R = 8.0 \times 10^6$.
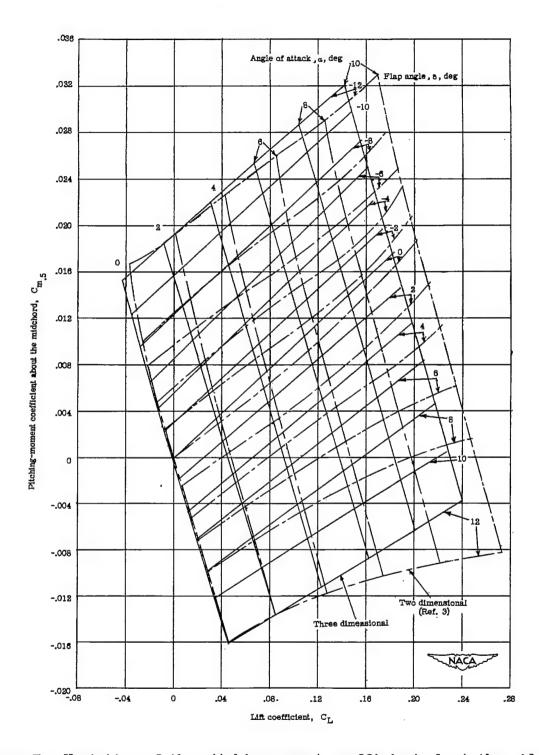
(b) Lift-coefficient variation with flap angle.

Figure 4.- Concluded.
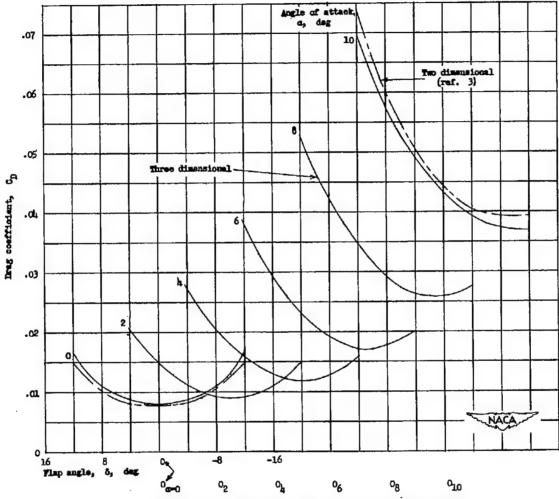
(a) Drag-coefficient variation with angle of attack.

Figure 5.- The variation of drag coefficient with angle of attack and flap angle for a rectangular wing of aspect ratio 1.33 having a 6-percent-thick circular-arc profile and a 30-percent-chord full-span trailing-edge flap. $M = 4.04$; $R = 8.0 \times 10^6$.

(b) Drag-coefficient variation with flap angle.

Figure 5.- Concluded.
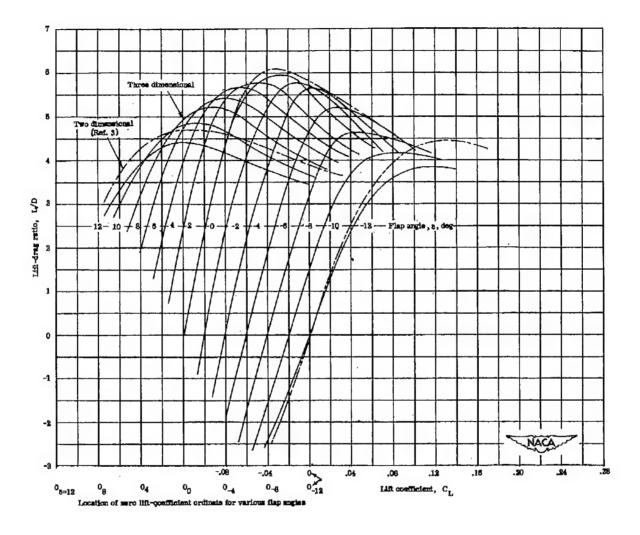
Figure 6.- The variation of lift-drag ratio with lift coefficient and flap angle for a rectangular wing of aspect ratio 1.33 having a 6-percent-thick circular-arc profile and a 30-percent-chord full-span trailing-edge flap. $M = 4.04$; $R = 8.0 \times 10^6$.
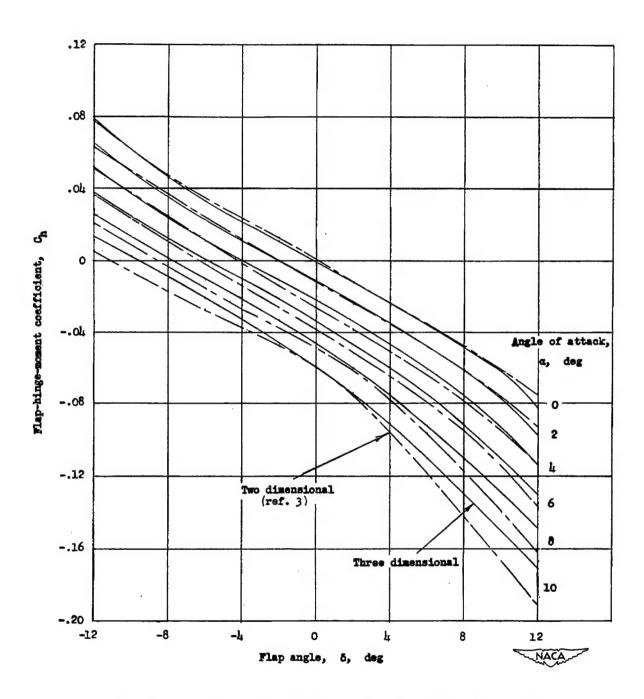
Figure 7.- Variation of the pitching-moment coefficient about the mid-
chord with lift coefficient and flap angle for a rectangular wing
of aspect ratio 1.33 having a 6-percent-thick circular-arc profile
and a 30-percent-chord full-span trailing-edge flap. M = 4.04;
R = 8.0 × 10⁶.
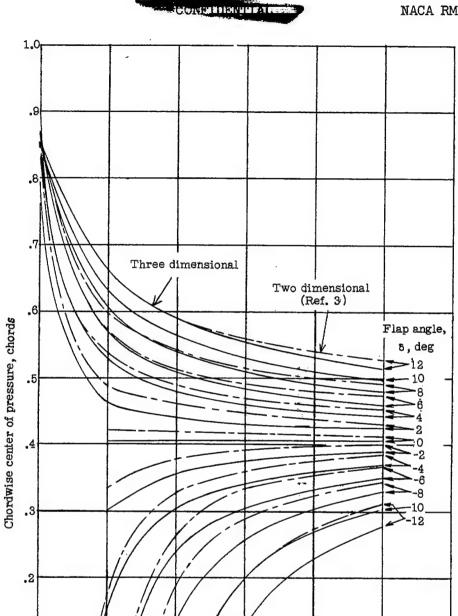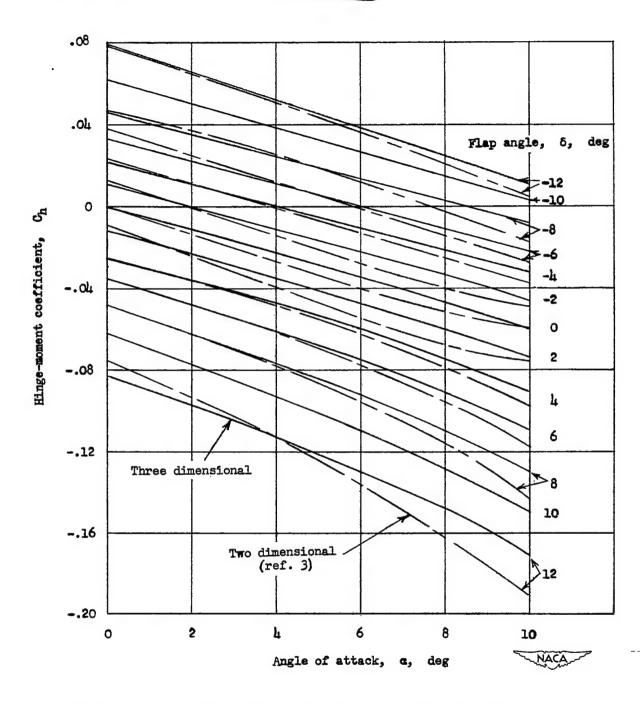
Figure 8.- Variation of the chordwise center of pressure from the leading
edge with angle of attack and flap angle for a rectangular wing of
aspect ratio 1.33 having a 6-percent-thick circular-arc profile and a
30-percent-chord full-span trailing-edge flap. M = 4.04; R = 8.0 × 10⁶.

(a) Hinge-moment coefficient variation with angle of attack.

Figure 9.- Variation of the hinge-moment coefficient with angle of attack
and flap angle for a rectangular wing of aspect ratio 1.33 having a
6-percent-thick circular-arc profile and a 30-percent-chord full-span
trailing-edge flap.　M = 4.04; R = 8.0 × 10⁶.

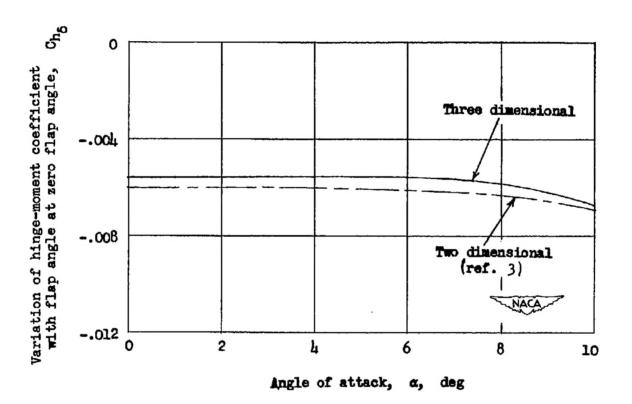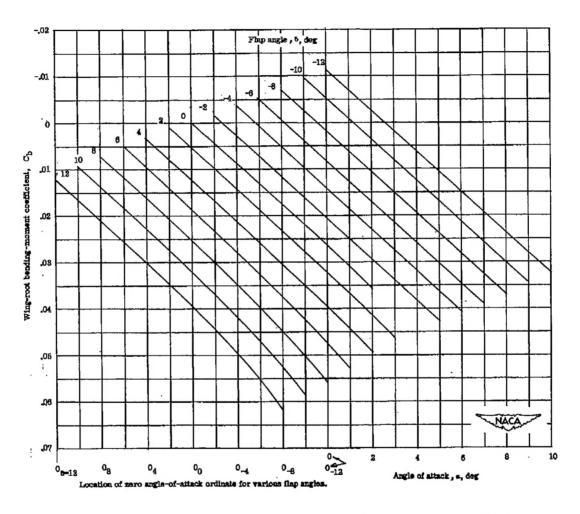(b) Hinge-moment coefficient variation with flap angle.

Figure 9.- Concluded.

Figure 10.- Variation of hinge-moment slope parameter with angle of
attack at zero flap angle for a rectangular wing of aspect ratio 1.33
having a 6-percent-thick circular-arc profile and a 30-percent-chord
full-span trailing-edge flap. $M = 4.04$; $R = 8.0 \times 10^6$.

Figure 11.- Variation of the wing-root bending-moment coefficient
with angle of attack and flap angle for a rectangular wing of
aspect ratio 1.33 having a 6-percent-thick circular-arc profile
and a 30-percent-chord full-span trailing-edge flap. $M = 4.04$;
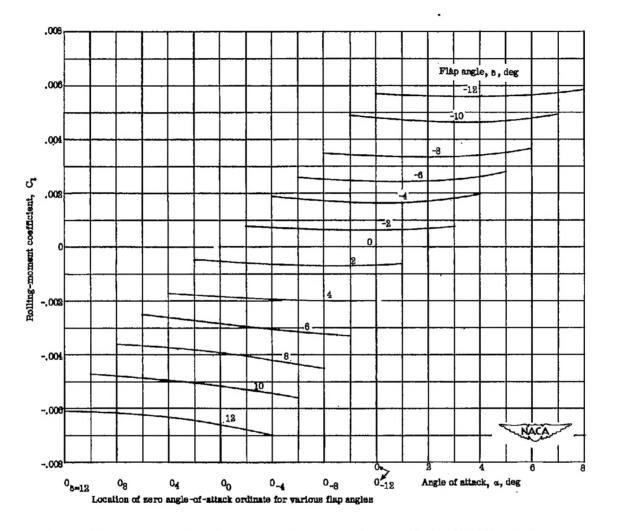$R = 8.0 \times 10^6$.

Figure 12.- Variation of the rolling-moment coefficient with angle of attack and flap angle for a rectangular wing of aspect ratio 1.33 having a 6-percent-thick circular-arc profile and a 30-percent-chord full-span trailing-edge flap. $M = 4.04$; $R = 8.0 \times 10^6$.
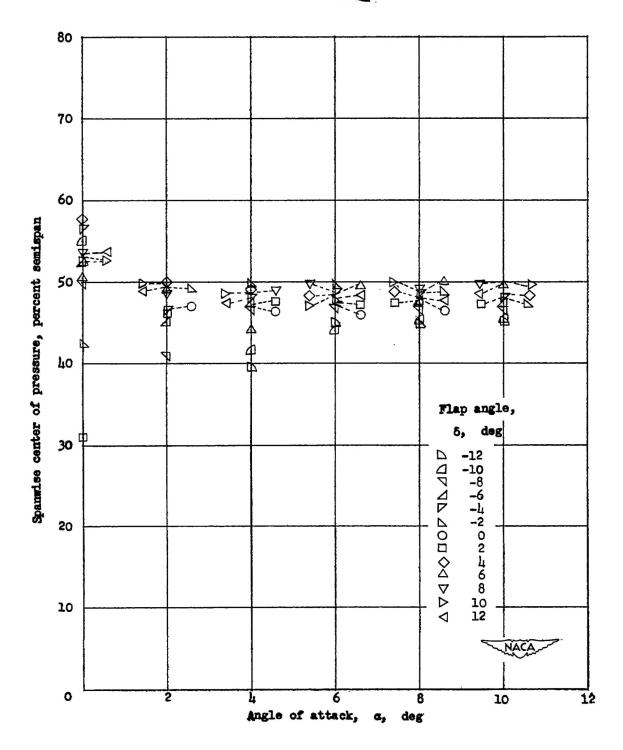
Figure 13.- Variation of the spanwise center of pressure with angle of
attack and flap angle for a rectangular wing of aspect ratio 1.33
having a 6-percent-thick circular-arc profile and a 30-percent-chord
full-span trailing-edge flap.   M = 4.04; R = 8.0 × 10⁶.